

Investigating properties of surfaces and thin films using microsphere whispering-gallery modes

A. T. Rosenberger*^a, E. B. Dale^a, D. Ganta^a, and J. P. Rezac^b

^aDepartment of Physics, Oklahoma State University, Stillwater, OK, USA 74078-3072

^bITT Advanced Engineering & Sciences, 5901 Indian School Rd. NE, Albuquerque, NM, USA 87110

ABSTRACT

We use a tunable diode laser operating near 1570 nm to investigate various effects of the heat transfer from fused-silica microspheres, with and without thin-film coatings, to the surrounding gas in a vacuum chamber. The resonance frequencies of microsphere whispering-gallery modes (WGMs), excited by a tapered-fiber coupler, shift with changing temperature (about -1.6 GHz/K at 1570 nm). This shift, primarily due to the temperature dependence of the refractive index of fused silica, enables the measurements whose results are reported here: determination of the thermal accommodation coefficient of air on different surfaces, and measurement of the optical absorption coefficients of surface water layers and of a thin film coating. Our method for determining thermal accommodation coefficients involves deducing the thermal conductivity of the air as a function of pressure by measuring the relaxation rate of an externally heated microsphere to room temperature. Then, in a separate experiment, by observing thermal optical bistability of the WGM resonances caused by absorption of the probe laser, the contribution of water or film absorption to the total loss is found.

Keywords: microspheres, whispering-gallery modes, thermal accommodation coefficient, thermal bistability, optical absorption coefficient, thin-film absorption characterization

1. INTRODUCTION

It is well known that the whispering-gallery modes (WGMs) of dielectric microresonators can serve as sensitive probes of their environment, through the environment's interaction with the WGMs' evanescent components. One example is microcavity-enhanced laser absorption spectroscopy of molecules in the ambient gas or liquid.^{1,2} Another effect that can be used as an environmental probe is the temperature sensitivity of WGM resonance frequencies.³⁻⁵ A high- Q microresonator can easily measure mK temperature changes; while this can be a complication for some applications, it can also be put to use in detecting heat absorbed and lost by the microresonator. At wavelengths around 1570 nm, the resonance frequency will shift down by approximately 1.6 GHz for each Kelvin increase in temperature, due primarily to the change in refractive index,⁶ to which is added the effect of thermal expansion.

The experiments reported here are extensions of some of our earlier work.⁷ First, a microsphere is heated by focusing a laser beam onto it; upon turnoff of the heating beam, the microsphere relaxes back to room temperature. From its relaxation rate, observed via the WGM frequency shift using a weak tunable diode laser, we can calculate the thermal conductivity of the surrounding air. Doing this for a range of pressures allows us to determine the thermal accommodation coefficient of air on the surface (roughly the probability that a gas molecule will equilibrate with the surface after one collision). The surface in these experiments is either bare fused silica or a polymer film coating. This is a novel method for measuring accommodation coefficients. In a second experiment, use of the diode laser at higher power (without an external heating beam) produces thermal bistability; since the previous experiment determined the heat loss, the bistability gives us the heat supplied by the fraction of total optical power lost due to absorption. This absorption results from a water layer on the surface of a bare sphere, and for a coated sphere it is due to the polymer film. The precision of these measurements is quite good ($\sim 5\%$), so the prospect of using these techniques for thin-film characterization is promising.

*atr@okstate.edu; phone 1 405 744-6742; fax 1 405 744-6811

2. EXPERIMENTS

The experimental setup is shown in Fig. 1. The microsphere is mounted in a cylindrical vacuum chamber that has a transparent top plate and side windows for viewing. The pressure in the chamber can be reduced from atmospheric to about 2 mTorr. Light from a cw tunable diode laser is coupled into a modulator, from which it exits into a single-mode optical fiber that passes through a polarization controller before being fed into the chamber, where its adiabatic bitapered region is brought into contact with the microsphere. The position and orientation of the coupling fiber are controlled, via bellows-sealed feedthroughs, by a positioner located outside the chamber. The polarization controller is adjusted to ensure that WGMs of a single polarization (TE or TM) are excited, and after the fiber is fed out of the chamber the two polarizations in the throughput can be detected separately. The modulator is normally off, but can be turned on to provide a square-wave intensity modulation; the throughput response to the square-wave input tells us whether a WGM is undercoupled or overcoupled (intrinsic or coupling loss dominant, respectively) without changing the geometry of the system. As seen in Fig. 1, the microsphere is actually a prolate spheroid of average radius about 300 μm , fabricated from optical fiber in such a way as to have very thin stems both above and below. The double stem helps to make the mounting more rigid, since the stems are so thin (tapering to just a few μm). The 532-nm heating beam of about 1 W comes from a frequency-doubled Nd:YVO₄ laser, and is focused through a side window onto the microsphere.

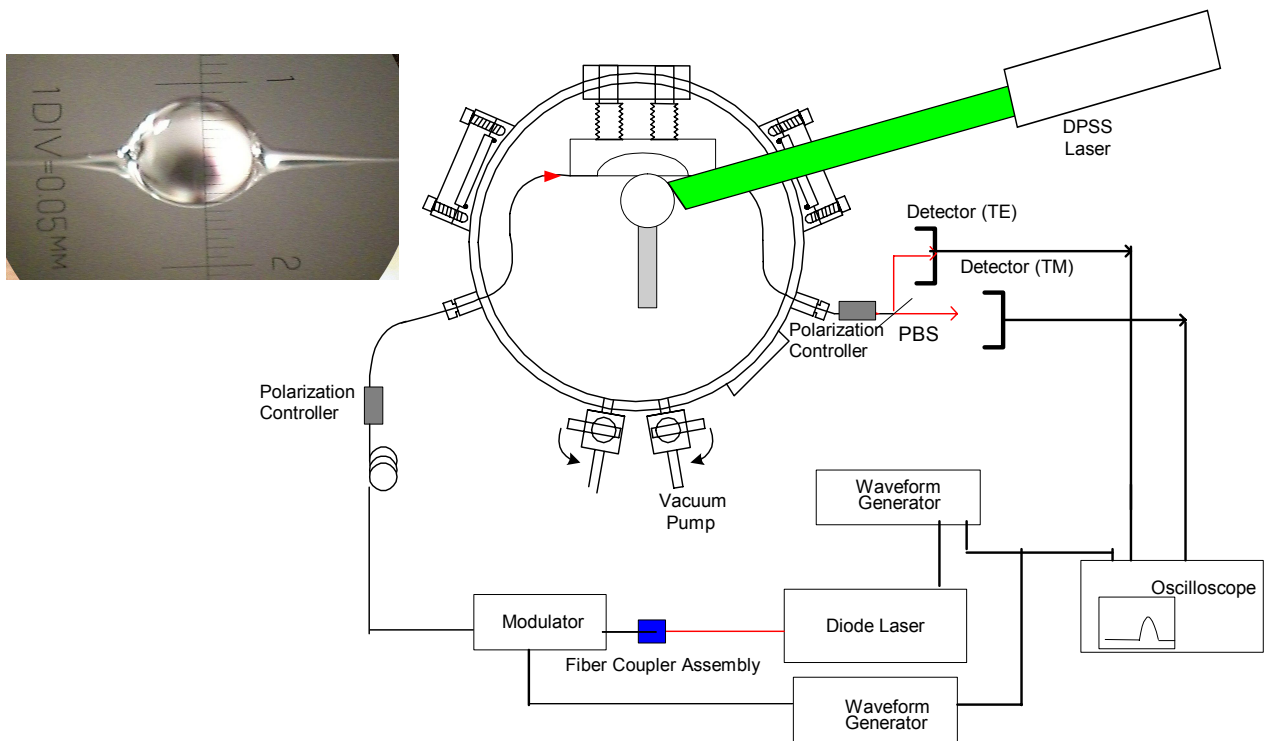


Fig. 1. Experimental setup. The diode laser is frequency-scanned by one waveform generator, while the other controls the modulation. The light couples from a tapered fiber into and back out of microsphere WGMs, and the throughput is detected. A polarizing beamsplitter (PBS) separates throughput of the two polarizations. A diode-pumped solid state laser can be used as an external heat source for the microsphere, and the vacuum chamber allows control over the ambient pressure. The inset at upper left shows a photograph of a microsphere with two thin stems.

The diode laser is scanned up and down in frequency by a triangle wave, so that the scan should be linear in time and have the same rate in both directions. In the thermal accommodation coefficient experiments, the external beam heats the microsphere to a few K above room temperature and is then turned off. The diode laser is kept at fairly low power ($\sim 7 \mu\text{W}$) so that it does not appreciably heat the microsphere. Displacement of a WGM's throughput dip from one scan trace to the next is analyzed to find the relaxation time constant as the microsphere returns to room temperature. Results from the two scan directions are averaged to reduce error due to residual scan nonlinearity. This is done over a wide range of pressures (about four orders of magnitude). The time constant provides the measured thermal conductivity of

the surrounding air, and fitting the thermal conductivity vs. pressure curve determines the thermal accommodation coefficient, as described in Section 3.

The thermal bistability experiments use the same system, minus the external heating laser. Now the diode laser power incident on the microsphere is on the order of 150 μW , so that the diode laser will heat the microsphere if it is scanned slowly enough across a WGM resonance. Since the relaxation time constant is known from the previous experiment, fitting the bistable throughput trace to a simple model will determine the single free parameter, which is the fraction of the total power loss that is due to absorption (assuming the absorbed power is converted to heat rather than reradiated). This is described in Section 4. Because the absorption in fused silica is so low in this wavelength range, we assume that all the absorption takes place in the water layer on the surface of the bare sphere, or in the polymer layer on the coated sphere. Then from the known absorption coefficient for bulk water, we can estimate the thickness of the water layer. Likewise, knowing the thickness of the polymer film, we can find its absorption coefficient.

3. ACCOMMODATION COEFFICIENTS

Analysis of these experiments is simplified by the fact that the thermal conductivity of fused silica is much greater than that of air. Therefore, the microsphere can be treated as being in thermal equilibrium (uniform internal temperature distribution) at all times because of its very fast internal relaxation.⁸ We assume that heat loss through the stems is negligible because of their small masses and long conduction paths. Because the microsphere is so small, convection is negligible,⁹ and so heat loss occurs through conduction by the surrounding air and by radiation. Define T to be the deviation of the microsphere's temperature above room temperature T_R , and the relaxation equation can be written as follows for $T \ll T_R$:

$$\frac{dT}{dt} = -\frac{1}{mc} \left(4\pi a k_{air} + 16\pi a^2 \varepsilon \sigma T_R^3 \right) T = -\frac{1}{\tau} T, \quad (1)$$

where m is the microsphere's mass, c is the specific heat of fused silica, a is the microsphere's radius, k_{air} is the measured thermal conductivity of air, ε is the emissivity of fused silica, σ is the Stefan-Boltzmann constant, and τ is the thermal relaxation time constant. Because the temperature variation is small, any temperature dependence of these parameters can be neglected. However, k_{air} will depend on pressure; the measured value will begin to decrease as the molecular mean free path becomes comparable to the size of the microsphere. The pressures used are such that our data are predominantly in the slip-flow or temperature-jump regime,¹⁰ that is, the pressure is higher than the free-molecular-flow regime. This means that the pressure dependence of k_{air} is given by

$$k_{air}(p) = \frac{k_{atm}}{1 + \left(\frac{2-\alpha}{\alpha} \right) \frac{k_{atm} \sqrt{2\pi R T_R}}{(c_p + c_v) p a}}. \quad (2)$$

In Eq. (2), k_{atm} is the thermal conductivity of air at atmospheric pressure, R is the gas constant per unit mass of air, c_p and c_v are the heat capacities of air at constant pressure and volume, respectively, p is the air pressure, and α is the thermal accommodation coefficient for air on the surface of interest. Fitting a plot of k_{air} vs. p then determines the value of α , the single free parameter.

Experimental values for k_{air} vs. p were found for two fused-silica microspheres, one bare (Fig. 2) and the other coated with a polyelectrolyte layer (Fig. 3). The second microsphere was dipped in a 0.5% solution of poly(dimethyldiallylammonium) chloride (PDDA) for about 30 minutes to produce a polyelectrolyte surface layer approximately 1 nm thick.¹¹ Because the microresonators were so prolate, an effective radius was chosen that gave the best fit of Eq. (2) to the data. For example, the bare sphere had a minor radius of 295 μm , a major radius of 375 μm , and an effective radius of $a = 325 \mu\text{m}$. Similarly, the PDDA-coated sphere had an effective radius of $a = 298 \mu\text{m}$. For the accommodation coefficient of air on fused silica, we find $\alpha = 0.84 \pm 0.03$, in good agreement with previous measurements for nitrogen and oxygen on glass.¹² Our value found for the accommodation coefficient of air on PDDA is $\alpha = 0.92 \pm 0.03$, slightly larger than on fused silica, as might be expected from the more porous structure of the PDDA surface.

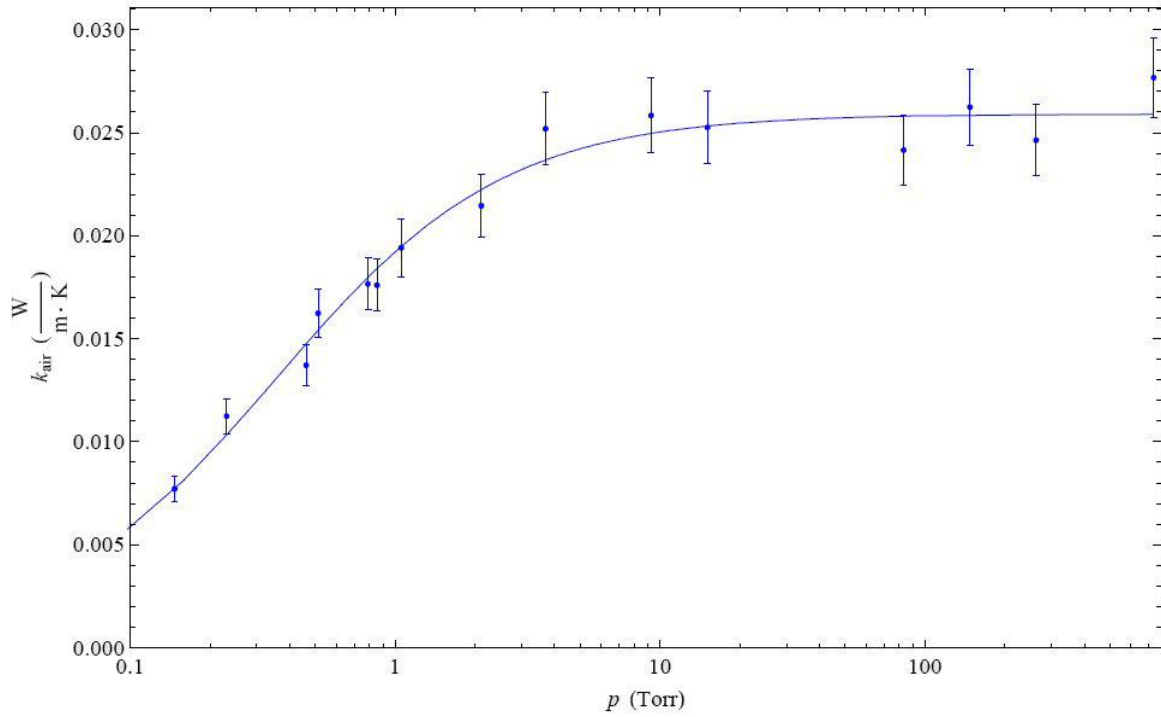


Fig. 2. Pressure dependence of thermal conductivity of air, measured using a bare microsphere of effective radius 325 μm . The fit to Eq. (2), shown as the curve, gives a thermal accommodation coefficient of 0.84 for air on fused silica.

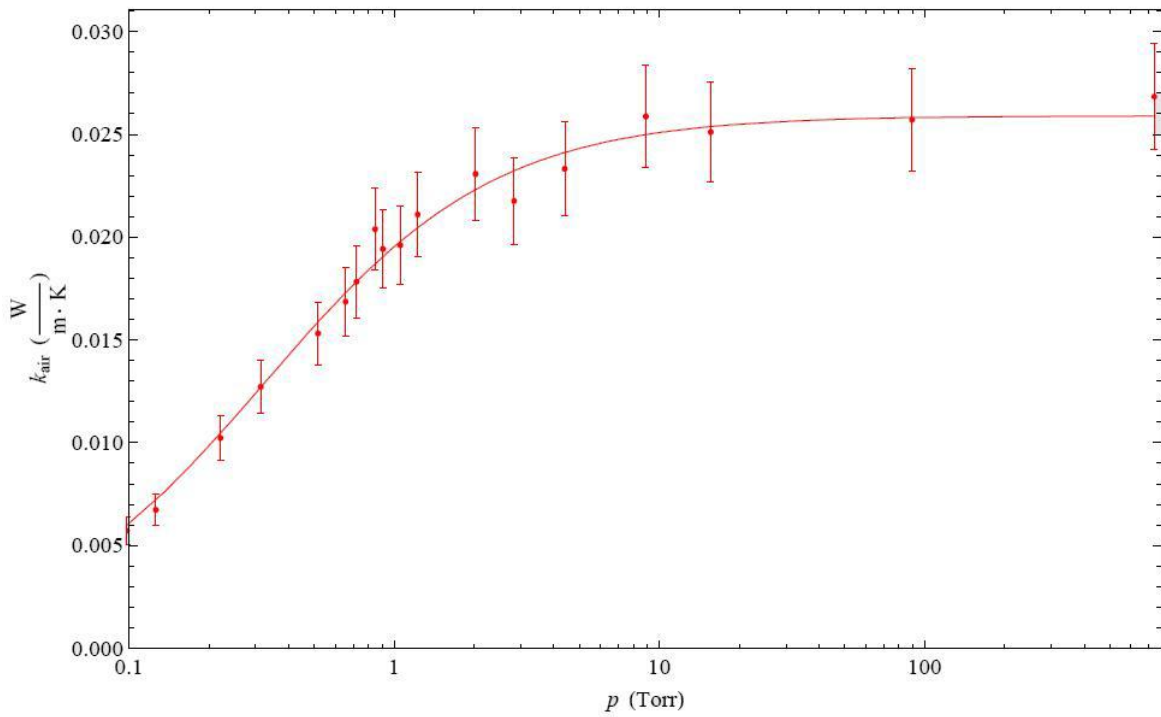


Fig. 3. Pressure dependence of thermal conductivity of air, measured using a PDDA-coated microsphere of effective radius 298 μm . The fit to Eq. (2), shown as the curve, gives a thermal accommodation coefficient of 0.92 for air on PDDA.

For the PDDA-coated sphere, since the coating thickness is much less than the effective radius, we use the specific heat of fused silica in Eq. (1). The emissivity of PDDA is not known, so the value for fused silica was used ($\varepsilon = 0.87$); the results are not sensitive to the exact value, because the radiation loss is smaller than the heat loss by conduction. Looking at the data in Figs. 2 and 3, no obvious effect of heat loss from the stems is seen. If stem loss were significant, the measured value of k_{air} would begin to fall off at a higher pressure than it does. Perhaps, however, the somewhat larger scatter and error in the data at high pressures may be a consequence of some stem loss, as well as residual heating by the diode laser. The fit of Eq. (2) to the data is quite sensitive to the value of α , so its error is only on the order of 3% despite the larger errors in k_{air} . The fit remains good even to the lowest pressures of 0.1 Torr, indicating that the transition to free-molecule behavior has not yet been seen. At even lower pressures, estimated for these spheres to be on the order of 10 mTorr,¹⁰ the data points should begin to fall below the curve of Eq. (2). This appears to be an entirely new method for measuring the accommodation coefficient; nothing similar is mentioned in the literature.¹²

4. THERMAL BISTABILITY

In these experiments, power absorbed from the diode laser coupled into a WGM, operating at higher power, heats the sphere. The laser is scanned slowly in frequency across a WGM resonance. The scan rate is slow enough that the assumption of internal thermal equilibrium in the microsphere holds, except perhaps during the fast throughput power jumps (see Figs. 4-7). In equilibrium, the power absorbed depends on the detuning from the temperature-dependent resonance, the depth of the resonance dip, and the power incident on the microsphere. Thus a heating term can be added to the right-hand side of Eq. (1) to describe the microsphere's temperature as a function of time:⁷

$$\frac{dT}{dt} = \frac{\beta M_0 P_{inc}}{mc} \frac{\left(\frac{\Delta\nu}{2}\right)^2}{(\nu(t) - \nu_0 + bT)^2 + \left(\frac{\Delta\nu}{2}\right)^2} - \frac{T}{\tau}, \quad (3)$$

where M_0 is the fractional dip depth,¹ P_{inc} is the power incident on the microsphere (and throughput off resonance), $\Delta\nu$ is the linewidth of the Lorentzian WGM resonance at $\nu_0 - bT$ where b is the 1.6 GHz/K temperature shift, and the only free parameter, β , is the fraction of the total power loss ($M_0 P_{inc}$) that is due to absorption. Fitting a throughput trace to a tuning curve derived from Eq. (3) gives the value of β . Now from $M_0 = 4x/(1+x)^2$, where the ratio of coupling to intrinsic losses is $x = T_c / 2\pi\alpha_i$, and the measured (loaded) quality factor

$$Q = \frac{\nu_0}{\Delta\nu} = \frac{2\pi n}{\lambda(1+x)\alpha_i}, \quad (4)$$

where n is the index of refraction of fused silica and λ is the wavelength, the intrinsic loss coefficient α_i can be found. There are two solutions, corresponding to the undercoupled ($x < 1$) and overcoupled ($x > 1$) cases, which is why the modulator is needed in the experiment to determine the coupling regime. Then the effective absorption coefficient is $\alpha_{abs} = \beta\alpha_i$. An approximate expression for the relation between the effective absorption coefficient of the water layer or thin film, of thickness δ , and its bulk absorption coefficient α_b has been given:¹³

$$\delta \cong \left(\frac{\lambda a}{\pi^5}\right)^{1/2} \frac{\alpha_{abs}}{4\alpha_b}. \quad (5)$$

Using Eq. (5) and the determined value of α_{abs} , we can estimate δ if α_b is known, and vice versa. Four examples of thermal bistability data, fit to a calculated tuning curve based on Eq. (3), are shown below. Figures 4 and 5 are for the bare sphere at two different pressures, and Figs. 6 and 7 are for the PDDA-coated sphere at two different pressures. In the figures, the laser scans slowly across a TM-polarized WGM resonance dip (taking at least several thermal relaxation times to scan $\Delta\nu$), first down in frequency, then reversing at the vertical dashed line and scanning back up in frequency across the same mode. The continuous smooth lines are the theoretical fits.

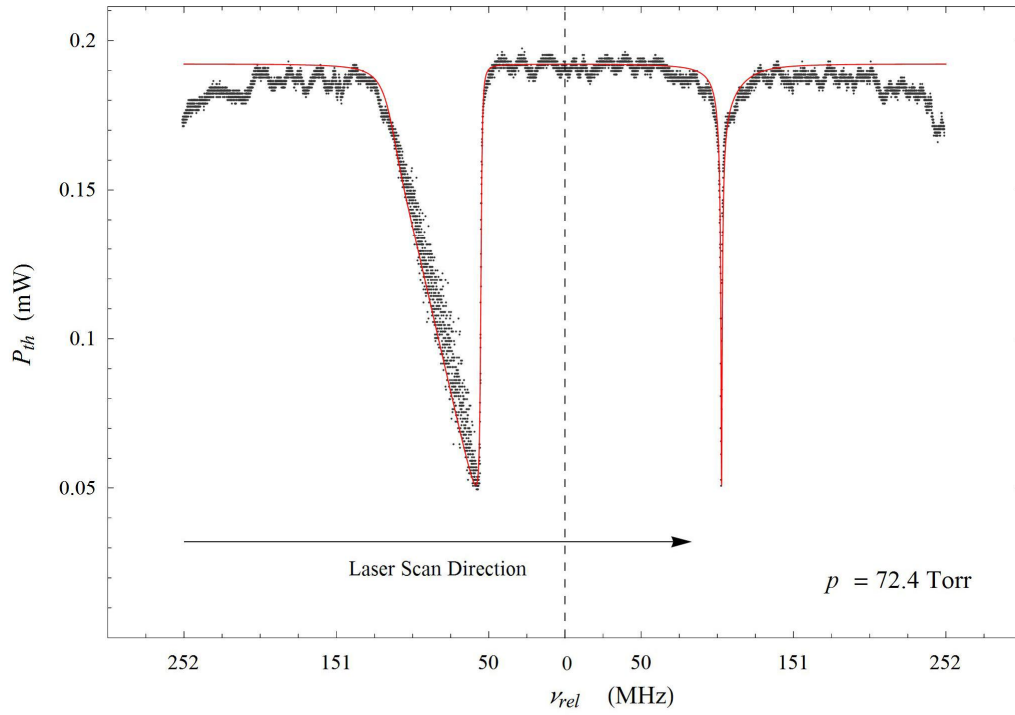


Fig. 4. WGM resonance dip showing thermal bistability. For this undercoupled mode in the bare sphere with $Q = 3.14 \times 10^7$, the fit gives $\alpha_{abs} = 0.00419 \text{ m}^{-1}$.

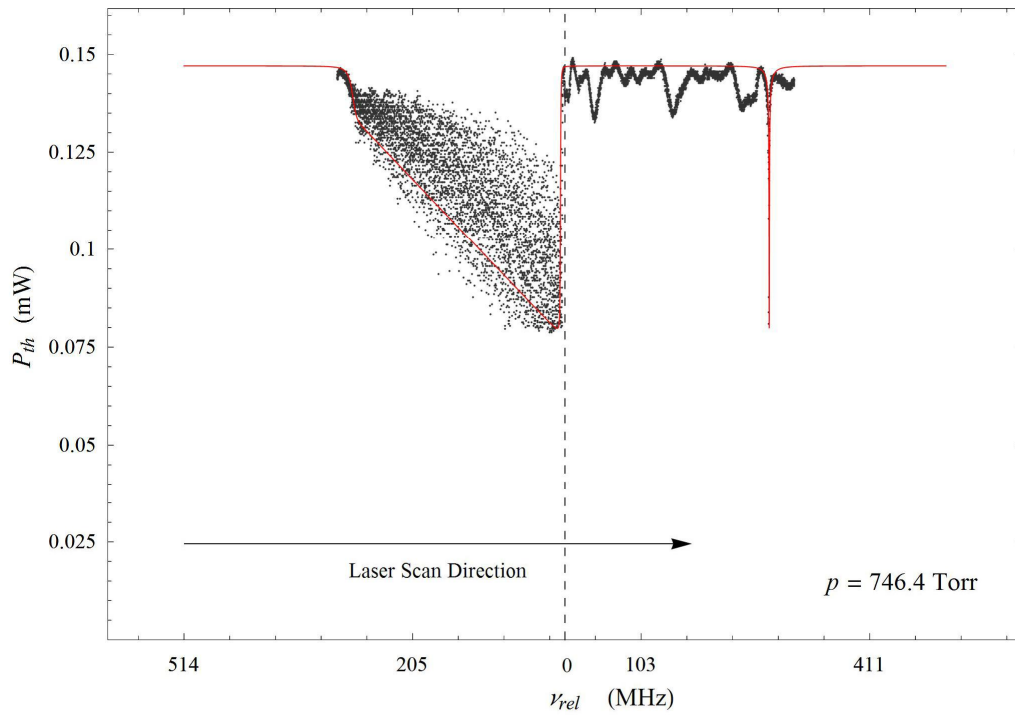


Fig. 5. WGM resonance dip showing thermal bistability. For this overcoupled mode in the bare sphere with $Q = 5.21 \times 10^7$, the fit gives $\alpha_{abs} = 0.00513 \text{ m}^{-1}$.

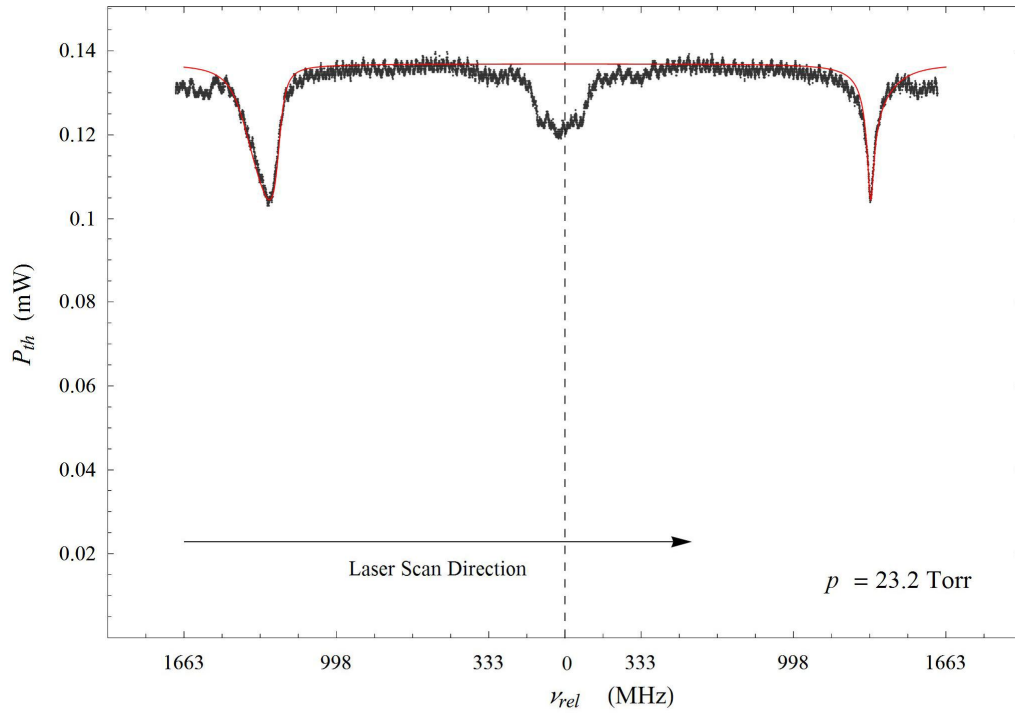


Fig. 6. WGM resonance dip showing thermal bistability. For this undercoupled mode in the PDDA-coated sphere with $Q = 2.15 \times 10^6$, the fit gives $\alpha_{abs} = 0.588 \text{ m}^{-1}$.

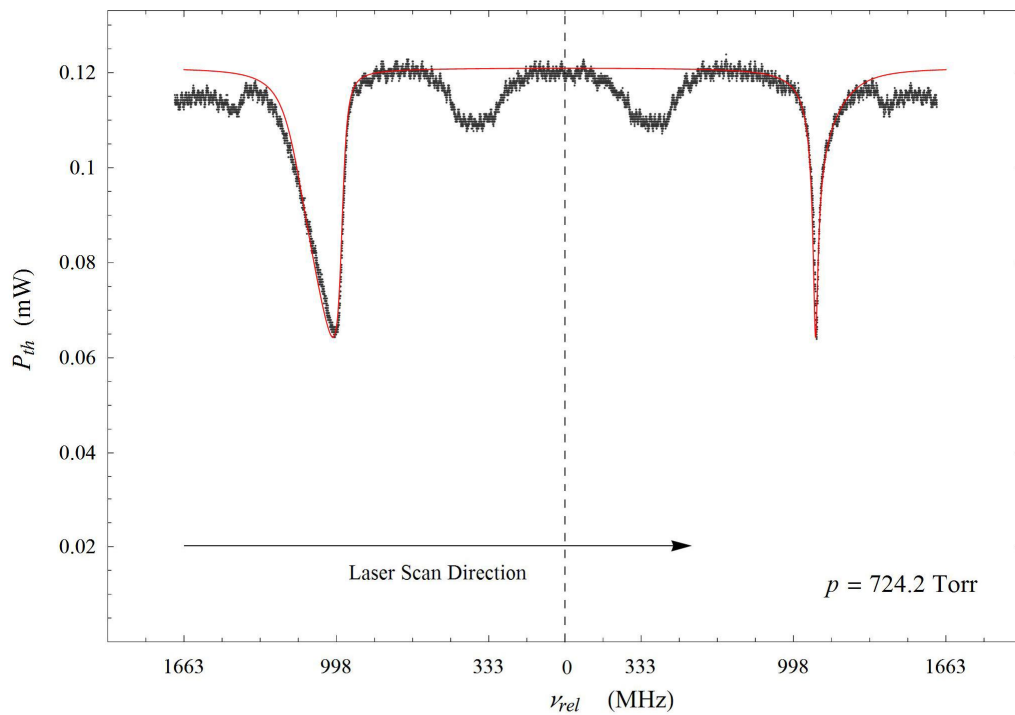


Fig. 7. WGM resonance dip showing thermal bistability. For this undercoupled mode in the PDDA-coated sphere with $Q = 2.25 \times 10^6$, the fit gives $\alpha_{abs} = 0.428 \text{ m}^{-1}$.

The fitting to the data in Figs. 4-7 gives the values of α_{abs} to about 5% precision. Note that the values for the bare sphere (Figs. 4 and 5) give values that are reasonably consistent despite the order of magnitude difference in pressures and the fact that one mode is undercoupled and the other overcoupled. Using Eq. (5) and the known bulk absorption coefficient of water (at these wavelengths, water has $\alpha_b \approx 800 \text{ m}^{-1}$),¹⁴ we estimate $\delta \approx 6.7 \text{ pm}$ from Fig. 4 and $\delta \approx 8.2 \text{ pm}$ from Fig. 5. These correspond to water coverage on the fused-silica surface of about 5-6% of a monolayer. A typical value is about one monolayer; our values may be lower than this because the sphere had been held at a low pressure for some time before the measurements were made. Applying the same analysis to Figs. 6 and 7, we estimate $\delta \approx 0.90 \text{ nm}$ from Fig. 6 and $\delta \approx 0.66 \text{ nm}$ from Fig. 7. These values indicate that the absorption coefficient of the PDDA film is of the same order of magnitude as that of bulk water.

5. CONCLUSIONS

The temperature sensitivity of the resonant frequencies of WGMs in a microsphere has been employed to measure the thermal conductivity of the ambient air as a function of pressure, and these results have enabled a quantitative explanation of thermal optical bistability observed in the microsphere under conditions of larger incident power. Measuring the thermal relaxation time to determine k_{air} vs. p , and fitting the results to the temperature-jump model of Eq. (2), determines the value of the thermal accommodation coefficient of air on the microsphere surface. Since these measurements can easily be done with various gases, using different surface coatings (thin compared to the wavelength), a large number of gas-surface interactions can be studied. This optical technique using microresonators is very well suited to making these measurements, and so adds a new method for the study of the interaction of gases with surfaces.

Measuring thermal bistability and fitting the observed mode profiles to the model, combined with the intensity modulation that permits determining the coupling regime without having to move any part of the setup, allows us to characterize the system losses.¹⁵ The coupling loss and intrinsic loss can be determined separately, and the intrinsic loss can be separated into its scattering and absorption components. The absorption component is predominantly due to the surface water layer on a bare sphere, or to the coating on a sphere to which a thin film has been applied. This technique then also permits the measurement of the absorption coefficient of the film, and it can be applied to films of any refractive index and absorption coefficient, provided only that the film is thin enough.

ACKNOWLEDGMENTS

Sarah Bates and Seth Koterba contributed to the initial experiments investigating these effects, and Razvan Stoian assisted with the PDDA coating. The vacuum chamber was constructed by Mike Lucas of the Physics/Chemistry Instrument Shop. This work has been supported by the National Science Foundation under award numbers 0329924 and 0601362, and by the Oklahoma Center for the Advancement of Science and Technology under project number AR072-066.

REFERENCES

- ¹ A. T. Rosenberger, "Analysis of whispering-gallery microcavity-enhanced chemical absorption sensors," *Opt. Express* **15**, 12959-12964 (2007).
- ² G. Farca, S. I. Shopova, and A. T. Rosenberger, "Cavity-enhanced laser absorption spectroscopy using microresonator whispering-gallery modes," *Opt. Express* **15**, 17443-17448 (2007).
- ³ V. S. Il'chenko and M. L. Gorodetskii, "Thermal nonlinear effects in optical whispering gallery microresonators," *Laser Physics* **2**, 1004-1009 (1992).
- ⁴ L. Collot, V. Lefèvre-Seguin, M. Brune, J.-M. Raimond and S. Haroche, "Very high-Q whispering-gallery mode resonances observed on fused silica microspheres," *Europhys. Lett.* **23**, 327-334 (1993).

- ⁵ T. Carmon, L. Yang, and K. J. Vahala, "Dynamical thermal behavior and thermal self-stability of microcavities," *Opt. Express* **12**, 4742-4750 (2004).
- ⁶ I. H. Malitson, "Interspecimen Comparison of the Refractive Index of Fused Silica," *J. Opt. Soc. Am.* **55**, 1205-1209 (1965).
- ⁷ J. P. Rezac, *Properties and Applications of Whispering-Gallery Mode Resonances in Fused Silica Microspheres*, PhD dissertation, Oklahoma State University, 2002.
- ⁸ H. S. Carslaw and J. C. Jaeger, *Conduction of Heat in Solids*, Clarendon, Oxford, 1959, Chap. IX, pp. 230-254.
- ⁹ W. R. Foss and E. J. Davis, "Transient Laser Heating of Single Solid Microspheres," *Chem. Eng. Commun.* **152-153**, 113-138 (1996).
- ¹⁰ E. H. Kennard, *Kinetic Theory of Gases*, McGraw-Hill, New York, 1938, Chap. VIII, pp. 291-337.
- ¹¹ A. L. Rogach, D. S. Koktysh, M. Harrison, and N. A. Kotov, "Layer-by-Layer Assembled Films of HgTe Nanocrystals with Strong Infrared Emission," *Chem. Mater.* **12**, 1526-1528 (2000).
- ¹² S. C. Saxena and R. K. Joshi, *Thermal Accommodation and Adsorption Coefficients of Gases*, Vol. II-1 of *McGraw-Hill/CINDAS Data Series on Material Properties*, Y. S. Touloukian and C. Y. Ho, eds., McGraw-Hill, New York, 1981.
- ¹³ D. W. Vernooy, V. S. Ilchenko, H. Mabuchi, E. W. Streed, and H. J. Kimble, "High-Q measurements of fused-silica microspheres in the near infrared," *Opt. Lett.* **23**, 247-249 (1998).
- ¹⁴ G. M. Hale and M. R. Querry, "Optical Constants of Water in the 200-nm to 200- μ m Wavelength Region," *Appl. Opt.* **12**, 555-563 (1973).
- ¹⁵ H. Rokhsari, S. M. Spillane, and K. J. Vahala, "Loss characterization in microcavities using the thermal bistability effect," *Appl. Phys. Lett.* **85**, 3029-3031 (2004).